Published in final edited form as:

Cancer Res. 2018 September 01; 78(17): 4839–4852. doi:10.1158/0008-5472.CAN-17-3629.

Erbin suppresses KSR1-mediated RAS/RAF signaling and tumorigenesis in colorectal cancer

Payton D. Stevens[1], **Yang-An Wen**[2], **Xiaopeng Xiong**[2], **Yekaterina Y. Zaytseva**[3], **Austin T. Li**[4], **Chi Wang**[2], **Ashley Stevens**[1], **Trevor N. Farmer**[2], **Tong Gan**[2,5], **Heidi L. Weiss**[2], **Masaki Inagaki**[6], **Sylvie Marchetto**[7], **Jean-Paul Borg**[7], and **Tianyan Gao**[1,2]

[1]Department of Molecular and Cellular Biochemistry, University of Kentucky, Lexington, KY, USA

[2]Markey Cancer Center, University of Kentucky, Lexington, KY, USA

[3]Department of Toxicology and Cancer Biology, University of Kentucky, Lexington, KY, USA

[4]Paul Laurence Dunbar High School, Lexington, KY, USA

[5]Department of Surgery, University of Kentucky

[6]Department of physiology, Mie University Graduate School of Medicine, Tsu, Mie, Japan

[7]Centre de Recherche en Cancérologie de Marseille (CRCM), 'Cell Polarity, Cell Signalling, and Cancer', Equipe Labellisée Ligue Contre le Cancer, Inserm, U1068, Marseille, F-13009, France; CNRS, UMR7258, Marseille, F-13009, France; Institut Paoli-Calmettes, Marseille, F-13009, France; Aix-Marseille University, UM 105, Marseille, F-13284, France

Abstract

Erbin belongs to the LAP (leucine-rich repeat and PDZ domain) family of scaffolding proteins that plays important roles in orchestrating cell signaling. Here we show that Erbin functions as a tumor suppressor in colorectal cancer (CRC). Analysis of Erbin expression in CRC patient specimens revealed that Erbin was downregulated at both mRNA and protein levels in tumor tissues. Knockdown of Erbin disrupted epithelial cell polarity and increased cell proliferation in 3D culture. In addition, silencing Erbin resulted in increased amplitude and duration of signaling through Akt and RAS/RAF pathways. Erbin loss induced epithelial-mesenchymal transition (EMT), which coincided with a significant increase in cell migration and invasion. Erbin interacted with kinase suppressor of Ras 1 (KSR1) and displaced it from the RAF/MEK/ERK complex to prevent signal propagation. Furthermore, genetic deletion of Erbin in Apc knockout mice promoted tumorigenesis and significantly reduced survival. Tumor organoids derived from Erbin/Apc double knockout mice displayed increased tumor initiation potential and activation of Wnt signaling. Results from gene set enrichment analysis (GSEA) revealed that Erbin expression associated positively with the E-cadherin adherens junction pathway and negatively with Wnt signaling in human CRC. Taken together, our study identifies Erbin as a negative regulator of tumor initiation and progression by suppressing Akt and RAS/RAF signaling in vivo.

Disclosure of Potential Conflicts of Interest

No potential conflicts of interest were disclosed.

Keywords

Erbin; tumor suppressor; epithelial-mesenchymal transition; epithelial cell polarity; colorectal cancer

INTRODUCTION

Erbin is a member of the leucine-rich repeat (LRR) and PDZ domain (LAP) protein superfamily. It contains multiple protein-protein interaction modules including 16 LRRs followed by a single PDZ domain at the C-terminus. Erbin is known to localize primarily to the adherens junctions and plays a role in maintaining the structural integrity of the junction in epithelial cells (1–3). The initial discovery of Erbin identifies Erbin as an ERBB2/Her2 receptor interacting protein that facilitates the localization of the receptor to the basolateral membrane of epithelial cells (4). In addition, it has been shown that Erbin attenuates RAF activation by disrupting Shoc2-mediated RAS/RAF interaction (5,6). Moreover, downregulation of Erbin results in resistance to anoikis in cervical cancer cells via activation of JAK/STAT signaling (7). However, the role of Erbin in regulating cell polarity and colorectal cancer (CRC) tumorigenesis and progression remains elusive.

It has been well documented that epithelial cells, including those in the gastrointestinal tract, become polarized during the differentiation process (8). The polarization process, characterized by the formation of specialized junctions between neighboring cells, also results in the segregation of two plasma membrane domains: the apical surface, facing the external medium and the basolateral surface, connected to adjacent cells and extracellular matrix (9). The apical and basolateral membranes are segregated by two highly organized junctions, tight junctions and adherens junctions; and the many proteins that compose these junctions are assembled at the site of cell-cell contacts (10–12). Previous studies have demonstrated that loss of cell polarity, through the disruption of these junctions, is associated with increased tumorigencity and accompanied by EMT (13–15). Therefore, the proper establishment of epithelial polarity allows cells to sense and to respond to signals that arise from the microenvironment in a spatiotemporally controlled manner.

By facilitating the assembly of tightly controlled signaling complexes through protein-protein interactions, scaffold proteins are known to play important roles in regulating spatiotemporal responses in cell signaling (16). One of the best-known examples is the signal propagation in the RAS/RAF pathway, where the step-by-step activation process from RAS to ERK is facilitated by scaffolding proteins, such as KSR and Shoc2 (17,18). KSR1, a kinase-like protein that lacks enzymatic activity, has been shown to promote cell proliferation and oncogenic potential by enhancing signaling activation through the RAS/RAF pathway (19). KSR1 binds constitutively to MEK in the cytoplasm in unstimulated cells and translocates to the plasma membrane upon RAS activation (20,21). At the plasma membrane, KSR1 facilitates signaling propagation by organizing the formation of RAF/MEK/ERK complex (21,22). Although the molecular mechanism by which scaffold proteins positively regulate RAS/RAF signaling has been extensively studied,

it remains largely unknown whether scaffolding proteins are involved in signaling termination.

Here, we report the identification of Erbin as a novel tumor suppressor in colon cancer. We show that the mRNA and protein expression of Erbin is markedly decreased in CRC patient specimens. Erbin negatively regulates RAS/RAF signaling by sequestering KSR1 and preventing the formation of KSR1/RAF1 complex. Functionally, knockdown of Erbin results in an increase in cell motility by inducing EMT in colon cancer cells, and deletion of Erbin gene significantly decreases the lifespan of Apc mutant mice and accelerates the tumor progression.

MATERIALS AND METHODS

Mice

All animal procedures were performed by following protocols approved by the University of Kentucky Institutional Animal Care and Use Committee. Erbin knockout mice on C57BL6 background as previously described (23) were maintained by random inter-crossing to sustain a heterogeneous mixed genetic background. To produce animals used in the experiments, Erbin$^{+/-}$ mice were bred with Apc$^{f/f}$ and Villin-cre (Vil-cre) mice (both were obtained from the Jackson Laboratory) on a C57BL6 background. These mice were then inter-crossed to produce three cohorts of animals, including Apc$^{f/+}$/Erbin$^{+/+}$/Vil-cre (Apc/WT), Apc$^{f/+}$/Erbin$^{+/-}$/Vil-cre (Apc/Het), and Apc$^{f/+}$/Erbin$^{-/-}$/Vil-cre (Apc/KO). To monitor survival, these cohorts of mice were followed for up to 6 months.

Cells and reagents

Caco2, HT29 and SW480 cells obtained from American Type Culture Collection (Manassas, VA) were cultured in Dulbecco's modified Eagle medium (DMEM) supplemented with 10% fetal bovine serum (FBS, Sigma-Aldrich) and 1% penicillin/streptomycin. LIM2405 obtained from Ludwig Cancer Research Institute were cultured in RPMI-1640 supplemented with 10% FBS, 2mM L-Glutamine, 25mM HEPES and 1% penicillin/streptomycin. The mutation status of common CRC-associated genes is specified in Supplementary Table S1 (24). Human colon cancer cell lines were authenticated using short tandem repeat (STR) DNA profiling and tested negative for mycoplasma using PCR in March 2016 (Genetica, OH, USA). Stable Erbin and KSR1 knockdown cells were generated by lentivirus-based shRNAs as previously described. (25–27). The shRNA targeting sequences for human Erbin are: 5'-GCAGCCAAGTACAACCGTTAA-3' (A1) and 5'-CGGGCTCAAGTTGCATTTGAA-3' (A2); and for mouse Erbin are: 5'-GTTGGATTCAAATCAGATAAA-3' (B1) and 5'- CAGTCACTACTCTAGATTATT-3' (B2). The shRNA targeting sequence for KSR1 is 5'-CAACAAGGAGTGGAATGATTT-3'. To generate WT and Erbin knockout MEF cells, Erbin heterozygous mice were used for breeding and individual embryos at day 13 of gestation were isolated and genotyped. MEF cells were produced from WT and Erbin null embryos by following standard protocols (28). The primary MEF cells were immortalized using retrovirus-mediated knockdown of p53 using pBabe-puro-shp53 (Addgene).

Transwell migration and invasion assay

Transwell migration and invasion assays were performed by following previously described procedures (25). Briefly, cells grown to 50% confluency were serum starved overnight. For migration assays, 50,000 cells were seeded into Transwells in 0.1% bovine serum albumin (BSA) and allowed to migrate for 4.5 h at 37°C towards serum-free DMEM containing collagen (15 μg/mL) and EGF (10 ng/mL). For the invasion assay, cells were seeded into the upper chambers of Transwells that were pre-coated with Matrigel (BD Biosciences). The cells were allowed to migrate toward 5% FBS in the lower chamber for 24 hours. At the end of the incubation period, cells migrated to the bottom of Transwells were fixed and stained with crystal violet. The numbers of cells were counted using an inverted microscope at 20X magnification.

Time-lapse live cell imaging and analysis

Control and Erbin knockdown Cells were serum starved for 4 hours and plated as single cells onto collagen (15 μg/mL) coated glass bottom culture dishes (MatTek). Cells were stimulated with EGF (10 ng/ml) and the trajectory of moving cells were captured using a Nikon BioStation IM equipped with a CO_2 incubation chamber. Time-lapse phase images were taken every 10 minutes for 6 hours with a 20X objective (25,29). The recorded movement of the cells was analyzed using Nikon Elements AR software.

Three-dimensional cell culture and immunofluorescence staining

The polarization process of Caco2 cells was examined by following procedures described previously (30). Briefly, single cell suspension of Caco2 cells were cultured in 3D matrix consisting of 50% growth-factor reduced Matrigel (BD Biosciences) and 50% Collagen I (Thermo Fisher Scientific). The cells were allowed to grow into acinar structures in the 3D matrix for 10 days. The phase-contrast images of the acini were captured using a Nikon Eclipse Ti-E inverted microscope. For immunofluorescence staining, the acini were fixed in 4% paraformaldehyde in PBS and permeabilized with 0.5% Triton X-100 in PBS. Actin was stained using Alexa 488-conjugated phalloidin while the nuclei of the cells were stained with DAPI-containing mounting medium. To detect proliferating cells, the cells grown in 3D culture were treated with 5-ethynyl-2´-deoxyuridine (EdU) for 1 h prior to fixation. The EdU positive cells were stained using Click-iT EdU Alexa Fluor 488 Imaging Kit (Thermo Fisher Scientific). Images were taken using an Olympus FlowView FV1000 confocal laser-scanning microscope (Olympus).

Western blot analysis

Colon cancer cells or mouse tumor organoids were harvested and detergent-solubilized cell lysates were obtained as described previously (25–27,31). Equal amounts of cell lysates were resolved by SDS-PAGE and subjected to western blot analysis. The Erbin antibody has been reported previously (3). The phospho-AKT (p-AKT for Ser473), pan-Akt, phospho-RAF1 (p-RAF1 for Ser338), total RAF1, phospho-MEK1/2 (p-MEK for Ser217/221), total MEK1/2, phospho-ERK1/2 (p-ERK for Thr202/Tyr204), total ERK1/2, and E-cadherin antibodies were from Cell Signaling. The vimentin and N-cadherin antibodies were from BD Biosciences. The β-actin and γ-tubulin antibodies were from Sigma-Aldrich.

Histologic analysis and immunohistochemical (IHC) staining

Mice were euthanized at indicated time-points when showing signs of intestinal neoplasia, such as hunched stature and rectal bleeding. Intestine segments were opened longitudinally onto filter paper and made into “Swiss-roll” preparations as described previously (25). For histological analysis, H&E sections were prepared from fixed and paraffin embedded Swiss-roll specimens by following standard techniques. The CRC tissue microarray was created by the Biospecimen Procurement and Translational Pathology Shared Resource Facility of the Markey Cancer Center, which contains 45 pairs of tumor and adjacent normal control tissues collected from CRC patients who had undergone surgery resections at the Markey Cancer Center. For IHC staining, tissue sections were deparaffinized, rehydrated, and treated with hydrogen peroxide. Antigen retrieval was performed using Dako Target Retrieval Solution (DakoCytomation), and IHC staining was performed as previously described (26). The stained sections were visualized using a Nikon Eclipse 80i upright microscope.

Isolation and culture of mouse tumor organoids

Intestinal tumors were isolated from three cohorts of Apc/Erbin compound mutant mice, including Apc/WT, Apc/Het and Apc/KO, cultured in 3D Matrigel as described previously (32,33). Dissociated tumor cells were embedded in 33% Matrigel in 3D growth medium [Advanced DMEM/F12 supplemented with 1×N-2, 1×B-27, 1 mmol/L *N*-acetylcysteine, EGF (50 ng/mL) and 1% penicillin/streptomycin]. Tumor organoids were allowed to grow for 5 days and collected for protein or RNA analysis. For colony formation assays, single cell suspensions of 1,000 cells derived from tumor organoids were seeded into 3D Matrigel as described above. The number of colonies formed after 5 days were counted using an inverted microscope.

Tumor organoids derived from $Apc^{f/+}/Kras^{LSL\text{-}G12D}$/Villin-Cre mice was generated and described previously (33). To silence Erbin expression, tumor organoids were dissociated into small cell clusters using TrypLE (Thermo) and incubated with sh-Erbin lentivirus in suspension for 6 hours in a 37°C incubator. Cells were subsequently embedded in 33% Matrigel in 3D growth medium (Advanced DMEM/F12 supplemented with 1×Glutamax, 1×N-2, 1×B-27, 1 mM N-Acetyl-L-cysteine and 1% penicillin/streptomycin), and puromycin was added 2 days later to select for stable knockdown cells. For colony formation assays, tumor organoids were dissociated and single cell suspensions were seeded into 3D Matrigel. The number of tumor organoids formed after 6 days were counted and analyzed using an inverted microscope.

Real-time PCR

Total RNA was isolated from mouse tumor organoids using the RNeasy Mini Kit (Qiagen, MD, USA). Equal amounts of RNA were used as templates for the synthesis of cDNA using RT^2 HT First Strand kit (Qiagen). Real-time PCR was performed using mouse *Lgr5*-, *Axin2*-*Cd44*-, *Ccnd1*-, *Ki67*-, *Alpi*-, *Fabp2*- and *Muc2*-specific probes using StepOne Real-Time PCR system (Applied Biosysems). All values were normalized to the level of β-actin. The overall expression of β-actin mRNA remained unchanged in different treatment groups as determined by the Ct (threshold cycle) values.

Bioinformatics and statistical analysis

In experiments to assess gene or protein expression, rate of cell migration, size and number of cell grown in 3D, and EdU incorporation were summarized using bar graphs and pairwise comparisons between different conditions were carried out using two-sample t-tests. To determine the relative expression of Erbin gene in human CRC patients, microarray and patient clinical data from two CRC studies were downloaded from the Oncomine database. The Cancer Genome Atlas (TCGA) dataset contains 192 adenocarcinoma and 22 normal samples, within which 13 were matched pairs. Expression of Erbin in tumor vs. normal samples was compared using linear mixed models. The Skrzypczak et al. dataset contains 81 tumors and 24 normal samples. Expression of Erbin in tumor vs. normal samples was compared based on 2-sample *t* test. All statistical analyses were performed using R (version 3.4.1).

For the Gene Set Enrichment Analysis (GSEA), RNA sequencing data were obtained from the TCGA Colorectal Cancer study. Correlations between expressions of ERBIN and the other genes was quantified by Spearman's correlation coefficient. The genes were then ordered from highest to lowest based on the correlation coefficient. This ranked list was inputted into the GSEA Desktop Application (34) to identify pathways that are associated with ERBIN expression.

RESULTS

Erbin is downregulated in CRC patient tumor samples

To determine if Erbin mRNA expression (gene symbol: *ERBIN*; previously known as ERBB2IP) is altered in CRC patients, we performed bioinformatic analysis of two microarray data sets of human CRC samples. The microarray and patient clinical data of the two studies (35,36) were downloaded from the Oncomine database. The mRNA expression of Erbin was significantly reduced in tumor samples when compared to normal controls (Fig 1A–B). Interestingly, additional analysis of Erbin expression in stage I-IV of CRC patients revealed that Erbin was downregulated upon tumor initiation when compared to normal controls and no further loss of Erbin mRNA was observed as tumors progressed through stage II-IV, thus suggesting that loss of Erbin expression is an early event in tumorigenesis (Supplementary Fig S1). Additionally, the expression of Erbin protein was detected along the epithelial cell-cell junction in normal human colon tissues by IHC staining, whereas the expression of Erbin was markedly reduced and mislocalized to cytoplasma in tumor tissues (Fig 1C). The basolateral distribution of Erbin in normal tissues was consistent with those observed previously (3,37). Quantitative results obtained from IHC staining of a CRC tissue microarray revealed that basolateral membrane localization of Erbin was lost in all CRC tumor tissues examined (Fig 1D and Supplementary Fig S1). Furthermore, we analyzed Erbin protein expression in matched normal and tumor tissues obtained from seven CRC patients using western blot. Consistent with IHC staining results, Erbin protein levels were significantly decreased in tumor tissues compared to normal controls (Fig 1E–F and Supplementary Fig S1). Collectively, our data obtained in patient samples provided the first evidence suggesting that Erbin may function as tumor suppressor in CRC.

Knockdown of Erbin increases both Akt and RAS/RAF signaling

Previous studies have implicated that Erbin negatively regulates ERK signaling (5,38). To determine the function of Erbin in CRC, we silenced Erbin expression using two shRNA lentiviral targeting constructs (A1 and A2) in SW480, LIM2405 and Caco2 colon cancer cell lines. Consistently, knockdown of Erbin resulted in an increase in phosphorylation and activation of both the Akt and MEK/ERK pathways in all three cell lines (Fig 2A). Since both Erbin shRNA targeting constructs had similar effects on silencing Erbin expression and enhancing activation of Akt and MEK/ERK phosphorylation, the subsequent experiments were mostly performed using sh-Erbin-A2 shRNA and key findings were confirmed with sh-Erbin-A1 shRNA. To further examine the effect of Erbin-loss on the temporal activation of signaling, stable control and Erbin knockdown SW480 cells were starved for 16 hours and subsequently stimulated with EGF for the indicated time (Fig 2B). Knockdown of Erbin increased both the amplitude and the duration of signaling through the Akt and RAF/MEK/ERK pathways (Fig 2C). Similar results were obtained in EGF-treated LIM2045 cells (Supplementary Fig S2).

Erbin is required to maintain cell polarity

We next investigated the functional effects of Erbin downregulation using a 3D cell culture system. Control and Erbin knockdown Caco2 and SW480 cells were seeded into 3D Matrigel and allowed to grow for 10 days to form tumor spheroids. As described in previous studies (30,39,40), control Caco2 cells were able to form acini-like spherical structures with a single hollow lumen, which consisted of a layer of polarized epithelial cells as indicated by the apical localization of F-actin (Fig 3A). In marked contrast, Erbin depletion altered the acinar structure by inducing the formation of multiple lumens (Fig 3A). Moreover, although not fully polarized, control SW480 cells were able to form tumor spheroids with partially hollowed lumens; however, cell clusters formed by Erbin knockdown SW480 cells lacked lumen structure and exhibited no apical or basolateral differentiation (Fig 3A). Together, these results suggested that Erbin plays an important role in maintaining epithelial polarity.

Furthermore, we found that knockdown of Erbin markedly increased the size of the spheroids in both Caco2 and SW480 cells (Fig 3B). To determine if decreased Erbin expression alters cell proliferation in 3D culture, tumor spheroids formed by control and Erbin knockdown SW480 cells were labeled with EdU to mark proliferating cells (Fig 3C). Quantitative results showed that loss of Erbin expression increased cell proliferating (Fig 3D). To determine the molecular mechanism by which Erbin-loss induces polarity defects and promotes cell proliferation in 3D culture, control and Erbin knockdown SW480 spheroids were collected and analyzed by Western blot. Interestingly, the morphological changes observed in sh-Erbin cells were accompanied by the downregulation of E-cadherin (an epithelial cell marker) and upregulation of vimentin and N-cadherin (markers of fibroblasts/mesenchymal cells), suggesting that Erbin knockdown cells had undergone EMT (Fig 3E). Notably, increases in both Akt and ERK activation were maintained in Erbin knockdown spheroids grown in 3D (Fig 3E). Collectively, these data suggested that downregulation of Erbin disrupts epithelial polarity and induces EMT.

Knockdown of Erbin promotes cell migration and invasion in colon cancer

As we have observed EMT-like phenotypes in Erbin knockdown colon cancer cells grown in 3D, we next determined the role of Erbin on regulating cell motility. The induction of EMT as indicated by downregulation of E-cadherin and upregulation of vimentin was confirmed in SW480 cells grown in regular 2D culture (Fig 4A). To monitor single cell motility, time-lapse images of control and Erbin knockdown SW480 and LIM2405 cells were captured and the distances traveled of individual cells were analyzed using Nikon BioStation. Results showed that Erbin knockdown cells were considerably more motile and average distances traveled by Erbin knockdown cells were significantly increased compared to the control cells (Fig 4B–C), suggesting that Erbin-loss increases cell motility at the single cell level.

In addition, control Erbin knockdown SW480 and LIM2405 cells were subjected to Transwell migration and invasion assays. We found that both Erbin knockdown SW480 and LIM2405 cells migrated significantly faster than the control cells (Fig 4D). Similarly, knockdown of Erbin in HT29 cells increased cell migration as determined using Transwell assays (Supplementary Fig S2); and silencing Erbin using two different targeting shRNAs had comparable effects on promoting migration in SW480 cells (Supplementary Fig 2). Furthermore, knockdown of Erbin significantly increased the ability of SW480 cells to invade through Matrigel (Fig 4E), thus confirming that loss of Erbin promotes cell migration and invasion. Since Erbin downregulation activates both Akt and ERK signaling, we further determined the functional contribution of these two pathways in regulating the cell motility downstream of Erbin. Interestingly, the effect of Erbin-loss on promoting cell migration was completely blocked by treating cells with MEK inhibitor (PD98059) whereas Akt inhibitor (MK2206) had no effect (Fig 4F). The effect of MEK and Akt inhibitors on suppressing ERK and Akt activation was confirmed using western blot analysis (Fig 4G). Collectively, these results suggested that increased cell migration observed in Erbin knockdown cells is likely a result of MEK/ERK signaling activation.

Erbin inhibits RAF/MEK/ERK signaling by disrupting the RAF1-KSR1 interaction

In our effort to further define the molecular mechanism underlying Erbin-mediated inhibition of MEF/ERK signaling, we identified KSR1 as an interacting protein of Erbin. KSR1 is known to facilitate the formation of RAF/MEK/ERK complex upon RAS activation (20). We performed co-immunoprecipitation experiments to determine if Erbin expression affects the interaction between KSR1 and RAF1. 293T cells transfected with Flag-RAF1 in the presence or absence of CFP-KSR1 and Myc-Erbin were immunoprecipitated with the anti-Flag antibody. The overexpressed and endogenous KSR1 were found to interact with RAF1 (Fig 5A). However, co-expression of Erbin largely reduced the amount of KSR1interacting with RAF1 (Fig 5A–B). In addition, the interaction between endogenous Erbin and KSR1 was readily detected in LIM2405 cells (Fig 5C). Importantly, knockdown of Erbin resulted in an increase in formation of KSR1-RAF1 complex in both Caco2 and LIM2405 cells (Fig 5D). Furthermore, we found that Erbin-loss induced increase in ERK activation was abolished in cells where KSR1 was also silenced (Fig 5E), thus confirming the functional interplay between Erbin and KSR1 in regulating RAF/MEK/ERK signaling. Collectively, these results suggest that Erbin functions to prevent KSR1 from forming a signaling complex with RAF1 and inhibit signaling activation downstream of RAF.

Genetic deletion of Erbin promotes tumorigenesis in Apc mutant mouse model

To determine the effect of Erbin-loss on tumorigenesis of CRC *in vivo*, we crossed Erbin-null mice with the $Apc^{f/f}$/Vil-cre mouse model (41) to investigate the susceptibility of mice deficient in Erbin to Apc-driven intestinal adenomas. Erbin knockout (KO) mouse models have been used in previous studies to investigate inflammatory responses, cardiac hypertrophy, and Her2/neu-mediated tumorigenesis in breast cancer (42–44). The Erbin KO mice did not develop spontaneous tumors. We compared the proliferation and differentiation of normal intestinal epithelial cells in WT and Erbin KO mice and found no difference in the number of proliferating cells and differentiated cells of different cell linages (Supplementary Fig S3). Consistently, the expression of genes associated with normal intestinal stem and differentiated cells remained unchanged in intestinal organoids derived from Erbin heterozygous and homozygous KO mice compared to WT mice (Supplementary Fig S4). However, consistent with results obtained in CRC cells, we found that the amplitude and duration of EGF-stimulated Akt and RAF/Mek/Erk signaling were largely increased in Erbin KO MEF cells (Supplementary Fig S4). Take together, these results suggest that Erbin-loss induced activation of Akt and Erk signaling alone is not sufficient to initiate tumorigenesis in colon cancer.

To specifically assess the role of Erbin in tumor initiation and progression in intestinal epithelium, we cross Erbin KO mice onto the Apc mutant background to generate the following three cohorts of mice: $Apc^{f/+}$/Vil-Cre/$Erbin^{+/+}$, $Apc^{f/+}$/Vil-Cre/$Erbin^{+/-}$ and $Apc^{f/+}$/Vil-Cre/$Erbin^{-/-}$ (Apc/WT, Apc/Het, and Apc/KO, respectively). The survival studies showed that knockout of a single allele of Erbin was sufficient to markedly accelerate the tumorigenesis process, resulting in a significantly shorter lifespan when compared to Apc/WT mice. Knockout of both alleles of Erbin further accelerated this process and significantly decreased survival (Fig 6A). Histopathological analysis revealed that adenomas were detected in both intestine and colon regions in all three cohorts of mice. However, when Apc/WT mice were sacrificed at time points that corresponded to average lifespan of Apc/KO mice (2 month), the difference in tumor burdens was particular clear in that more than half of Apc/KO mice reached the maximum tumor burden at 2 month when no tumors were detected in Apc/WT mice (Fig 6B). The increased tumor burden was observed in Apc/Het mice sacrificed at 4.5 month (the average lifespan of this cohort) when compared to Apc/WT mice of same age, although to a less extent (Supplementary Fig S5). At the terminal stage of tumor development (i.e. the mice were sacrificed due to tumor burden), the total numbers and size of tumors in all three cohorts were not significantly different. Thus, deletion of each Erbin allele significantly shortened the time needed to reach maximal tumor burden in a gene dosage-dependent manner.

To determine the effect of Erbin-loss on signaling activation *in vivo*, intestinal tumor tissues from Apc/WT, Apc/Het, and Apc/KO mice were analyzed for the phosphorylation of Akt and Erk using IHC staining. Since the tumorigenesis time course for Apc/KO mice was drastically accelerated in which no tumors were observed in Apc/WT mice at 2 months when majority of Apc/KO mice died (Fig 6A–B), we collected tumor tissues from different cohorts of mice when they reached maximal tumor burden. Consistently, the levels of Akt and Erk phosphorylation were markedly increased in Apc/Het and Apc/KO tumors

compared to Apc/WT (Fig 6C). Additionally, tumor cells isolated from Apc/WT and Apc/KO mice were allowed to grow into tumor organoids in 3D Matrigel. These organoids comprised of adenoma cells form cystic structure without budding (Fig 6D). To determine if Erbin inhibits signaling in mouse adenomas, protein lysates prepared from tumor organoids were subjected to western blot analysis. Both Akt and Erk phosphorylation were markedly increased in Erbin KO organoids (Fig 6E). Together, these data showed that Erbin-loss promotes the activation of Akt and Erk signaling and tumorigenesis in mouse models of CRC.

Loss of Erbin increases the tumor initiation potential of Apc tumor organoids

We next analyzed the tumor initiation capacity of mouse tumor organoids using the colony formation assay. Apc/WT and Apc/KO organoids were dissociated into single cells and re-seeded into Matrigel. The number of tumor organoids formed was counted after 5 days in culture. Knockout of Erbin resulted in a two-fold increase in organoid formation (Fig 7A), suggesting increased tumor initiation capacity. In addition, we determined the profile of gene expression using quantitative RT-PCR analysis in tumor organoids. Apc/WT and Apc/KO organoids grown in 3D culture for 5 days were collected and analyzed for the expression of Wnt target genes that are known to associate with cancer stem cells (eg. Lgr5, Axin2, and Cd44), intestinal cell differentiation (eg. Alpi, Fabp2, and Muc2), and cell proliferation (eg. Ccnd1 and Ki67). Tumor organoids derived from Apc/KO mice expressed higher levels of genes associated with Wnt signaling and cell proliferation, which coincided with decreased expression of genes associated with differentiated intestinal epithelial cells (Fig 7B). Similarly, the expression of genes associated with Wnt signaling and cell proliferation were significantly increased and intestinal differentiation decreased in tumor organoids derived from Apc/Het mice (Supplementary Fig S5), confirming that haplodeficiency of Erbin is sufficient to promote tumorigenesis.

Intriguingly, Erbin-loss did not result in EMT-like phenotypes as the expression of E-cadherin remained unchanged in Apc/KO tumor tissues and organoids compared to Apc/WT (data not shown). Since human colon cancer cells used in this study contain additional oncogenic alterations (such as KRAS or BRAF mutation), we performed additional experiments using Apc/Kras^{G12D} double mutant mouse tumor organoids to determine the effect of Erbin downregulation. Indeed, silencing Erbin using two different lentiviral shRNAs in Apc/Kras^{G12D} tumor organoids resulted in a decrease in E-cadherin expression and an increase in the phosphorylation of Akt and Erk (Fig 7C). Additionally, consistent with results obtained in Apc/KO organoids, the ability of Erbin knockdown Apc/Kras^{G12D} cells to form tumor organoids in 3D was increased (Fig. 7D), suggesting that decreased expression of Erbin promotes tumor initiation potential in Apc/Kras^{G12D} tumors as well.

Furthermore, we determined if Erbin expression is associated with cancer-related biological pathways by analyzing gene expression data from the Cancer Genome Atlas (TCGA) CRC RNA-seq dataset. Results from the Gene Set Enrichment Analysis (GSEA) showed Erbin expression is positively associated with the E-cadherin adherens junction (AJ) pathway and negatively associated with Wnt signaling (Fig 7E). These data support our findings that loss of Erbin promotes the disruption of epithelial polarity by reducing E-cadherin expression

and enhances tumor initiation potential by increasing signaling through the Wnt pathway. Taken together, our results showed that genetic deletion of Erbin potentiates tumor formation and progression *in vivo*.

DISCUSSION

Loss of epithelial polarity is a hallmark of advanced malignant tumors. Emerging evidence supports the notion that disruption of polarity promotes the malignant transformation of epithelial cells (14,45,46). In this study, combining *in vitro* and *in vivo* analyses we identify Erbin as a tumor suppressor in CRC. The mRNA expression of Erbin is significantly downregulated in CRC patients. Knockdown of Erbin in colon cancer cells results in disruption of epithelial polarity, increased cell motility and cell proliferation. Mechanistically, Erbin inhibits the activation RAF/MEK/ERK signaling by sequestering KSR1 from forming a complex with RAF1. Finally, our *in vivo* studies reveal that Erbin-loss accelerates tumor progression in Apc mutant mouse models.

Previous studies have suggested that Erbin inhibits the activation of ERK by disrupting Shoc2-mediated RAS/RAF interaction (5,6). However, Shoc2 is primarily localized to the endosome compartment of the cell (47). It remains an open question how Erbin, a basolateral membrane localized protein, interferes with Shoc2-dependent activation of RAS/RAF signaling at the endosome. In our study, we show that Erbin decreases RAF/MEK/ERK signaling through directly competing with KSR1. KSR1 is known to translocate to the plasma membrane upon RAS activation (20,21). Results from our study and others demonstrate that Erbin is localized at the basolateral membrane. Being in close proximity with receptor tyrosine kinases (such as EGFR) and the site of RAS activation, the presence of Erbin may block the access of KSR1 to RAS-bound RAF and reduces KSR1-RAF interaction. It is interesting that Erbin downregulation promotes further activation of ERK signaling cascade in CRC cells that contain KRAS or BRAF mutations. Thus, by providing a spatial control of how signaling complexes are assembled, Erbin may serve as a negative scaffold to restrict signaling output of oncogenic pathways mediated by wild-type or mutant KRAS and BRAF. Although the increased cell motility is mainly associated with activation of MEK/ERK pathway in Erbin knockdown cells, the activation of both Akt and MEK/ERK signaling likely contributes to increased tumorigenesis in Erbin knockout mice. It has been shown recently that oncogenic KRAS promotes Wnt signaling through ERK-mediated phosphorylation of LRP6 (48). However, treating Apc/KO tumor organoids with MEK or Akt inhibitor was unable to downregulate Wnt target gene expression in our study (data not shown). It is possible that loss of Erbin expression may alter the organization of epithelial junctions that allows the dissociation of β-catenin from the cell membrane. Future studies are required to determine the mechanism by which Erbin-loss induces activation of Wnt signaling.

The role of Erbin in cancer has been controversial. While a number of studies have shown that Erbin negatively regulates cell proliferation and survival in different types of cancer cells (7,49), other studies indicate that Erbin-loss increases tumorigenesis (44,50). Results from our study have provided several lines of evidence supporting the tumor suppressor function of Erbin in CRC: i) analysis of human CRC gene expression datasets with large

sample sizes indicates that Erbin mRNA expression is significantly downregulated in CRC patients; ii) Erbin protein expression is decreased in CRC patient specimens by western blot and IHC analyses; iii) knockout of Erbin in Apc mutant mice promotes tumor progression and reduces survival; and iv) tumor organoids derived from Erbin KO mice have increased tumor initiation potential. Our findings are also corroborated by the bioinformatics analysis in which Erbin expression is found to be downregulated at early stage of CRC and associated with increased E-cadherin junctions and decreased Wnt signaling. Additional gene sets that related to receptor tyrosine kinase signaling, cell cycle control and protein translation are identified to be associated with Erbin expression in CRC patients in our GSEA study (Supplementary Table S2), suggesting that Erbin-loss may have a broad impact on altering cell functions in cancer. Moreover, a number of missense, nonsense and frame-shift mutations are identified through out the entire coding region of Erbin based on an analysis of CRC datasets available at cBioPortal (Supplementary Fig S6) (51). The mutation rate of Erbin is between 2–4% among different studies. However, future studies are needed to determine the mechanism by which Erbin is downregulated in CRC and how Erbin-loss induces polarity defect and EMT.

In summary, our study has uncovered a pivotal role of Erbin in maintaining epithelial cell polarity and suppressing EMT in CRC. By developing novel *in vivo* mouse models and tumor organoid systems, we demonstrate that Erbin exerts its tumor suppressor function by negatively regulating both Akt and RAF/MEK/ERK signaling and Erbin-loss promotes tumor initiation and progression. The functional interplay between Erbin-KSR1 highlights the importance of scaffolding proteins in providing the spatiotemporal control of cell signals. Future studies on Erbin-dependent inhibition of tumor progression will help to explore the potential of using Erbin as a diagnostic marker for developing personalized treatment strategies in CRC.

Supplementary Material

Refer to Web version on PubMed Central for supplementary material.

Acknowledgements

We thank Dr. Emilia Galperin (University of Kentucky) for providing the expression construct of CFP-KSR1. This work was supported by R01CA133429 (TG) and F31 CA196219 (PDS). The studies were conducted with support provided by the Biospecimen Procurement and Translational Pathology and Biostatistics and Bioinformatics Shared Resource Facilities of the University of Kentucky Markey Cancer Center (P30CA177558). JP Borg's lab is funded by La Ligue Nationale Contre le Cancer (Label Ligue J.P.B.), Fondation A*MIDEX and SIRIC (INCa-DGOS-Inserm 6038). JPB is a scholar of Institut Universitaire de France.

References:

1. Favre B, Fontao L, Koster J, Shafaatian R, Jaunin F, Saurat JH, et al. The hemidesmosomal protein bullous pemphigoid antigen 1 and the integrin beta 4 subunit bind to ERBIN. Molecular cloning of multiple alternative splice variants of ERBIN and analysis of their tissue expression. The Journal of biological chemistry 2001;276(35):32427–36. [PubMed: 11375975]
2. Jaulin-Bastard F, Arsanto JP, Le Bivic A, Navarro C, Vely F, Saito H, et al. Interaction between Erbin and a Catenin-related protein in epithelial cells. J Biol Chem 2002;277(4):2869–75. [PubMed: 11711544]

3. Izawa I, Nishizawa M, Tomono Y, Ohtakara K, Takahashi T, Inagaki M. ERBIN associates with p0071, an armadillo protein, at cell-cell junctions of epithelial cells. Genes Cells 2002;7(5):475–85. [PubMed: 12047349]
4. Borg JP, Marchetto S, Le Bivic A, Ollendorff V, Jaulin-Bastard F, Saito H, et al. ERBIN: a basolateral PDZ protein that interacts with the mammalian ERBB2/HER2 receptor. Nat Cell Biol 2000;2(7):407–14. [PubMed: 10878805]
5. Huang YZ, Zang M, Xiong WC, Luo Z, Mei L. Erbin suppresses the MAP kinase pathway. J Biol Chem 2003;278(2):1108–14. [PubMed: 12379659]
6. Dai P, Xiong WC, Mei L. Erbin inhibits RAF activation by disrupting the sur-8-Ras-Raf complex. J Biol Chem 2006;281(2):927–33. [PubMed: 16301319]
7. Hu Y, Chen H, Duan C, Liu D, Qian L, Yang Z, et al. Deficiency of Erbin induces resistance of cervical cancer cells to anoikis in a STAT3-dependent manner. Oncogenesis 2013;2:e52. [PubMed: 23774064]
8. Bissell MJ, Radisky D. Putting tumours in context. Nat Rev Cancer 2001;1(1):46–54. [PubMed: 11900251]
9. Assemat E, Bazellieres E, Pallesi-Pocachard E, Le Bivic A, Massey-Harroche D. Polarity complex proteins. Biochim Biophys Acta 2008;1778(3):614–30. [PubMed: 18005931]
10. Kemler R Classical cadherins. Semin Cell Biol 1992;3(3):149–55. [PubMed: 1623204]
11. Fleming TP, Papenbrock T, Fesenko I, Hausen P, Sheth B. Assembly of tight junctions during early vertebrate development. Semin Cell Dev Biol 2000;11(4):291–9. [PubMed: 10966863]
12. Baas AF, Smit L, Clevers H. LKB1 tumor suppressor protein: PARtaker in cell polarity. Trends Cell Biol 2004;14(6):312–9. [PubMed: 15183188]
13. Huber MA, Kraut N, Beug H. Molecular requirements for epithelial-mesenchymal transition during tumor progression. Curr Opin Cell Biol 2005;17(5):548–58. [PubMed: 16098727]
14. Martin-Belmonte F, Perez-Moreno M. Epithelial cell polarity, stem cells and cancer. Nat Rev Cancer 2012;12(1):23–38.
15. Wodarz A, Nathke I. Cell polarity in development and cancer. Nat Cell Biol 2007;9(9):1016–24. [PubMed: 17762893]
16. Good MC, Zalatan JG, Lim WA. Scaffold proteins: hubs for controlling the flow of cellular information. Science 2011;332(6030):680–6. [PubMed: 21551057]
17. McKay MM, Morrison DK. Integrating signals from RTKs to ERK/MAPK. Oncogene 2007;26(22):3113–21. [PubMed: 17496910]
18. Wimmer R, Baccarini M. Partner exchange: protein-protein interactions in the Raf pathway. Trends Biochem Sci 2010;35(12):660–8. [PubMed: 20621483]
19. Kortum RL, Lewis RE. The molecular scaffold KSR1 regulates the proliferative and oncogenic potential of cells. Molecular and cellular biology 2004;24(10):4407–16. [PubMed: 15121859]
20. Stewart S, Sundaram M, Zhang Y, Lee J, Han M, Guan KL. Kinase suppressor of Ras forms a multiprotein signaling complex and modulates MEK localization. Molecular and cellular biology 1999;19(8):5523–34. [PubMed: 10409742]
21. Morrison DK. KSR: a MAPK scaffold of the Ras pathway? J Cell Sci 2001;114(Pt 9):1609–12. [PubMed: 11309192]
22. Michaud NR, Therrien M, Cacace A, Edsall LC, Spiegel S, Rubin GM, et al. KSR stimulates Raf-1 activity in a kinase-independent manner. Proceedings of the National Academy of Sciences of the United States of America 1997;94(24):12792–6. [PubMed: 9371754]
23. Tao Y, Dai P, Liu Y, Marchetto S, Xiong WC, Borg JP, et al. Erbin regulates NRG1 signaling and myelination. Proc Natl Acad Sci U S A 2009;106(23):9477–82. [PubMed: 19458253]
24. Mouradov D, Sloggett C, Jorissen RN, Love CG, Li S, Burgess AW, et al. Colorectal cancer cell lines are representative models of the main molecular subtypes of primary cancer. Cancer Res 2014;74(12):3238–47. [PubMed: 24755471]
25. Li X, Stevens PD, Liu J, Yang H, Wang W, Wang C, et al. PHLPP is a negative regulator of RAF1, which reduces colorectal cancer cell motility and prevents tumor progression in mice. Gastroenterology 2014;146(5):1301–12 e1–10. [PubMed: 24530606]

26. Liu J, Weiss HL, Rychahou P, Jackson LN, Evers BM, Gao T. Loss of PHLPP expression in colon cancer: role in proliferation and tumorigenesis. Oncogene 2009;28(7):994–1004. [PubMed: 19079341]
27. Wen YA, Stevens PD, Gasser ML, Andrei R, Gao T. Downregulation of PHLPP expression contributes to hypoxia-induced resistance to chemotherapy in colon cancer cells. Mol Cell Biol 2013;33(22):4594–605. [PubMed: 24061475]
28. Liu J, Stevens PD, Li X, Schmidt MD, Gao T. PHLPP-Mediated Dephosphorylation of S6K1 Inhibits Protein Translation and Cell Growth. Mol Cell Biol 2011;31(24):4917–27. [PubMed: 21986499]
29. Larson Y, Liu J, Stevens PD, Li X, Li J, Evers BM, et al. Tuberous sclerosis complex 2 (TSC2) regulates cell migration and polarity through activation of CDC42 and RAC1. J Biol Chem 2010;285(32):24987–98. [PubMed: 20530489]
30. Xiong X, Li X, Wen YA, Gao T. Pleckstrin Homology (PH) Domain Leucine-rich Repeat Protein Phosphatase Controls Cell Polarity by Negatively Regulating the Activity of Atypical Protein Kinase C. J Biol Chem 2016;291(48):25167–78. [PubMed: 27760826]
31. Wen YA, Li X, Goretsky T, Weiss HL, Barrett TA, Gao T. Loss of PHLPP protects against colitis by inhibiting intestinal epithelial cell apoptosis. Biochim Biophys Acta 2015;1852(10 Pt A):2013–23. [PubMed: 26187040]
32. Sato T, Stange DE, Ferrante M, Vries RG, Van Es JH, Van den Brink S, et al. Long-term expansion of epithelial organoids from human colon, adenoma, adenocarcinoma, and Barrett's epithelium. Gastroenterology 2011;141(5):1762–72. [PubMed: 21889923]
33. Wen YA, Xing X, Harris JW, Zaytseva YY, Mitov MI, Napier DL, et al. Adipocytes activate mitochondrial fatty acid oxidation and autophagy to promote tumor growth in colon cancer. Cell death & disease 2017;8(2):e2593. [PubMed: 28151470]
34. Subramanian A, Tamayo P, Mootha VK, Mukherjee S, Ebert BL, Gillette MA, et al. Gene set enrichment analysis: a knowledge-based approach for interpreting genome-wide expression profiles. Proc Natl Acad Sci U S A 2005;102(43):15545–50. [PubMed: 16199517]
35. Skrzypczak M, Goryca K, Rubel T, Paziewska A, Mikula M, Jarosz D, et al. Modeling oncogenic signaling in colon tumors by multidirectional analyses of microarray data directed for maximization of analytical reliability. PLoS One 2010;5(10):pii: e13091. [PubMed: 20957034]
36. Network TR. The Cancer Genome Atlas http://cancergenomenihgov/.
37. Legouis R, Jaulin-Bastard F, Schott S, Navarro C, Borg JP, Labouesse M. Basolateral targeting by leucine-rich repeat domains in epithelial cells. Embo Rep 2003;4(11):1096–102. [PubMed: 14578922]
38. Rangwala R, Banine F, Borg JP, Sherman LS. Erbin regulates mitogen-activated protein (MAP) kinase activation and MAP kinase-dependent interactions between Merlin and adherens junction protein complexes in Schwann cells. The Journal of biological chemistry 2005;280(12):11790–7. [PubMed: 15659388]
39. Jaffe AB, Kaji N, Durgan J, Hall A. Cdc42 controls spindle orientation to position the apical surface during epithelial morphogenesis. J Cell Biol 2008;183(4):625–33. [PubMed: 19001128]
40. Magudia K, Lahoz A, Hall A. K-Ras and B-Raf oncogenes inhibit colon epithelial polarity establishment through up-regulation of c-myc. J Cell Biol 2012;198(2):185–94. [PubMed: 22826122]
41. Cheung AF, Carter AM, Kostova KK, Woodruff JF, Crowley D, Bronson RT, et al. Complete deletion of Apc results in severe polyposis in mice. Oncogene 2010;29(12):1857–64. [PubMed: 20010873]
42. McDonald C, Chen FF, Ollendorff V, Ogura Y, Marchetto S, Lecine P, et al. A role for Erbin in the regulation of Nod2-dependent NF-kappaB signaling. The Journal of biological chemistry 2005;280(48):40301–9. [PubMed: 16203728]
43. Rachmin I, Tshori S, Smith Y, Oppenheim A, Marchetto S, Kay G, et al. Erbin is a negative modulator of cardiac hypertrophy. Proceedings of the National Academy of Sciences of the United States of America 2014;111(16):5902–7. [PubMed: 24711380]

44. Tao Y, Shen C, Luo S, Traore W, Marchetto S, Santoni MJ, et al. Role of Erbin in ErbB2-dependent breast tumor growth. Proc Natl Acad Sci U S A 2014;111(42):E4429–38. [PubMed: 25288731]

45. Huang L, Muthuswamy SK. Polarity protein alterations in carcinoma: a focus on emerging roles for polarity regulators. Curr Opin Genet Dev 2010;20(1):41–50. [PubMed: 20093003]

46. Royer C, Lu X. Epithelial cell polarity: a major gatekeeper against cancer? Cell Death Differ 2011;18(9):1470–7. [PubMed: 21617693]

47. Jang ER, Jang H, Shi P, Popa G, Jeoung M, Galperin E. Spatial control of Shoc2-scaffold-mediated ERK1/2 signaling requires remodeling activity of the ATPase PSMC5. J Cell Sci 2015;128(23):4428–41. [PubMed: 26519477]

48. Lemieux E, Cagnol S, Beaudry K, Carrier J, Rivard N. Oncogenic KRAS signalling promotes the Wnt/beta-catenin pathway through LRP6 in colorectal cancer. Oncogene 2015;34(38):4914–27. [PubMed: 25500543]

49. Liu D, Shi M, Duan C, Chen H, Hu Y, Yang Z, et al. Downregulation of Erbin in Her2-overexpressing breast cancer cells promotes cell migration and induces trastuzumab resistance. Mol Immunol 2013;56(1–2):104–12. [PubMed: 23711387]

50. Yao S, Zheng P, Wu H, Song LM, Ying XF, Xing C, et al. Erbin interacts with c-Cbl and promotes tumourigenesis and tumour growth in colorectal cancer by preventing c-Cbl-mediated ubiquitination and down-regulation of EGFR. J Pathol 2015;236(1):65–77. [PubMed: 25521828]

51. Gao J, Aksoy BA, Dogrusoz U, Dresdner G, Gross B, Sumer SO, et al. Integrative analysis of complex cancer genomics and clinical profiles using the cBioPortal. Sci Signal 2013;6(269):pl1.

SIGNIFICANCE:

Our findings establish the scaffold protein Erbin as a negative regulator of EMT and tumorigenesis in colorectal cancer through direct suppression of Akt and RAS/RAF signaling.

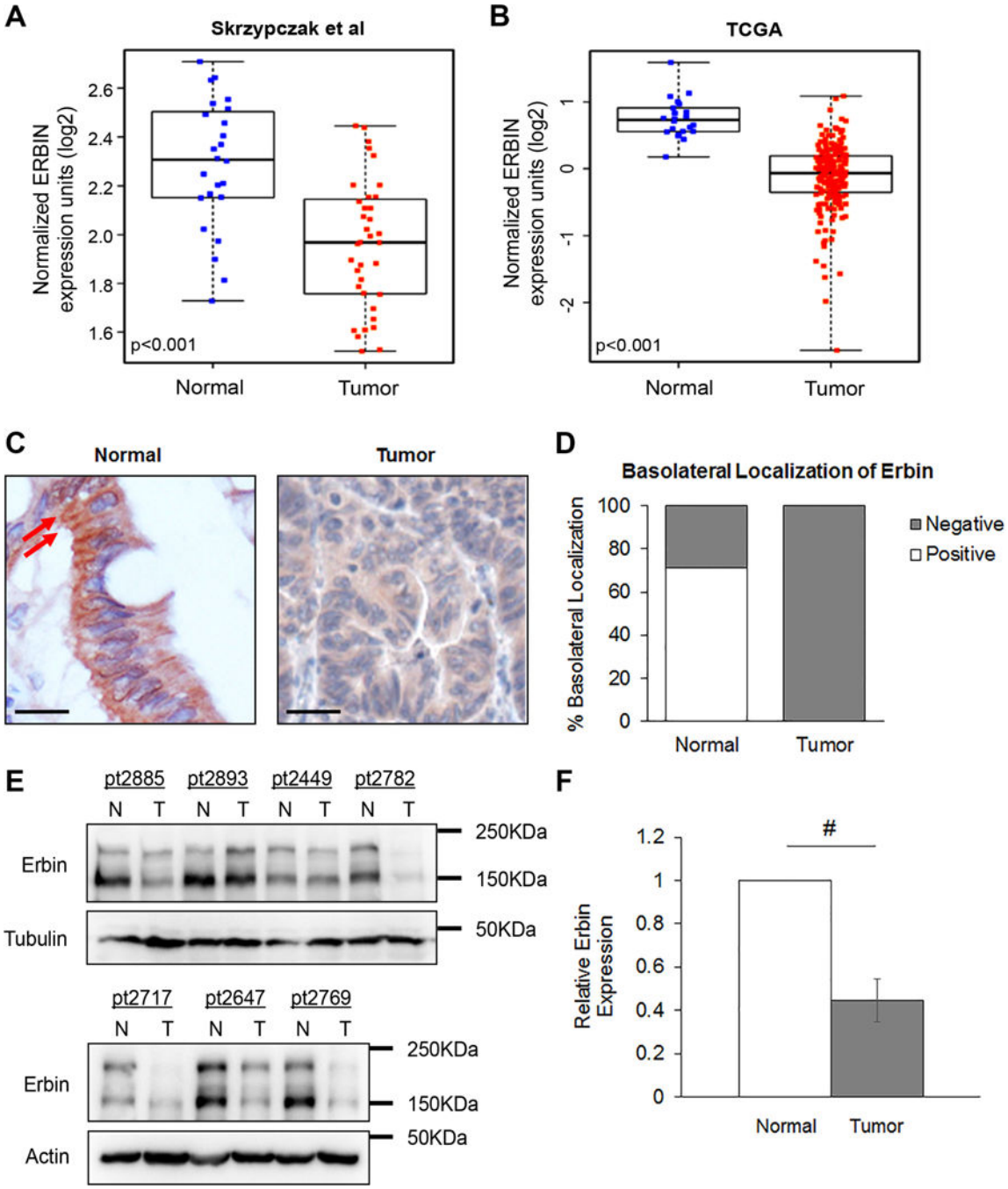

Figure 1. Erbin is downregulated and mislocalized in CRC patient samples.

(A) and (B) Microarray and patient clinical data from two colorectal cancer studies were downloaded from the Oncomine database (35,36). Data from Skrzypczak et al (35) (A) contained 24 normal and 36 adenocarcinoma samples; data from TCGA (B) contained 22 normal and 192 adenocarcinoma samples. Two-sample t-tests or linear mixed models were used to compare ERBIN gene expression between adenocarcinoma and normal samples ($p < 0.001$). (C) The expression of Erbin protein was detected in a tissue microarray (TMA) using IHC staining. The TMA contains 45 pairs of matched normal and tumor tissues. The

basolateral localization of Erbin was detected in normal colonic epithelial cells as indicated by red arrows. Scale bar, 50μm. (D) Bar graph depicts the percentage of basolateral localization of Erbin in both normal and tumor tissues (n=45). (E) Matched normal and tumor tissues from seven CRC patients were analyzed for Erbin expression using western blot. (F) The expression of Erbin protein was quantified by normalizing to tubulin or actin. The relative Erbin levels in tumor tissues were compared to that of normal tissues within the same patient. Data represents the mean ± SEM (# $p<0.0001$).

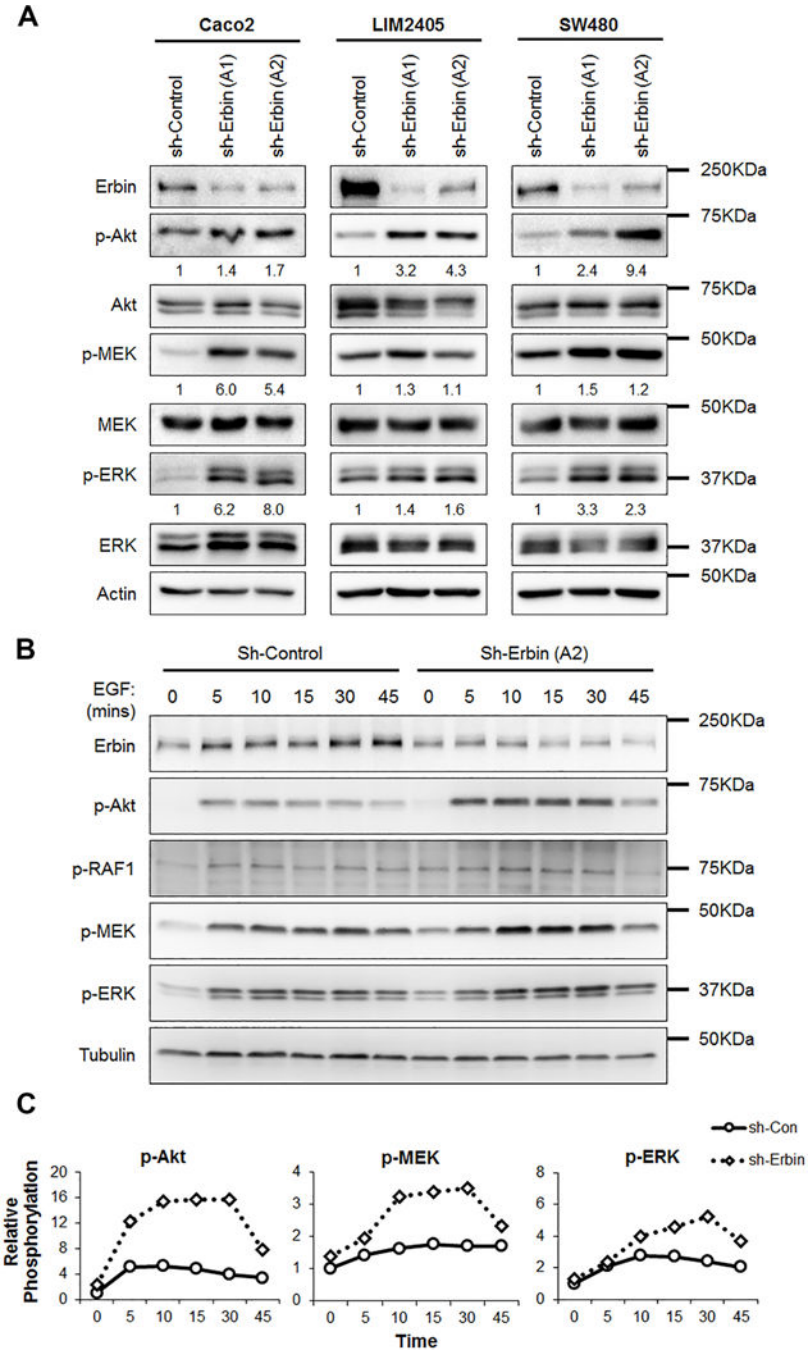

Figure 2. Knockdown of Erbin in CRC cells increases Akt and RAS/RAF signaling.

(A) Cell lysates prepared from stable control (sh-Control) and Erbin knockdown (sh-Erbin) cells, including Caco2, LIM2405 and SW480, were analyzed for the expression of Erbin and the phosphorylation status of Akt, MEK and ERK using Western blot. Two different shRNA targeting sequences (A1 and A2) were used to silence Erbin in each cell line. The relative phosphorylation of Akt, MEK and ERK was quantified by normalizing ECL signals generated by the phospho-specific antibodies to that of total proteins. (B) The stable control and Erbin knockdown SW480 cells were stimulated with EGF (10 ng/mL) for the indicated

times and activation of signaling molecules were analyzed using Western blot. (C) The relative levels of p-Akt, p-MEK and p-ERK in sh-Control and sh-Erbin SW480cell lines were quantified by normalizing ECL signals generated by the phospho-specific antibodies to that of total proteins and plotted over the EGF stimulation time course.

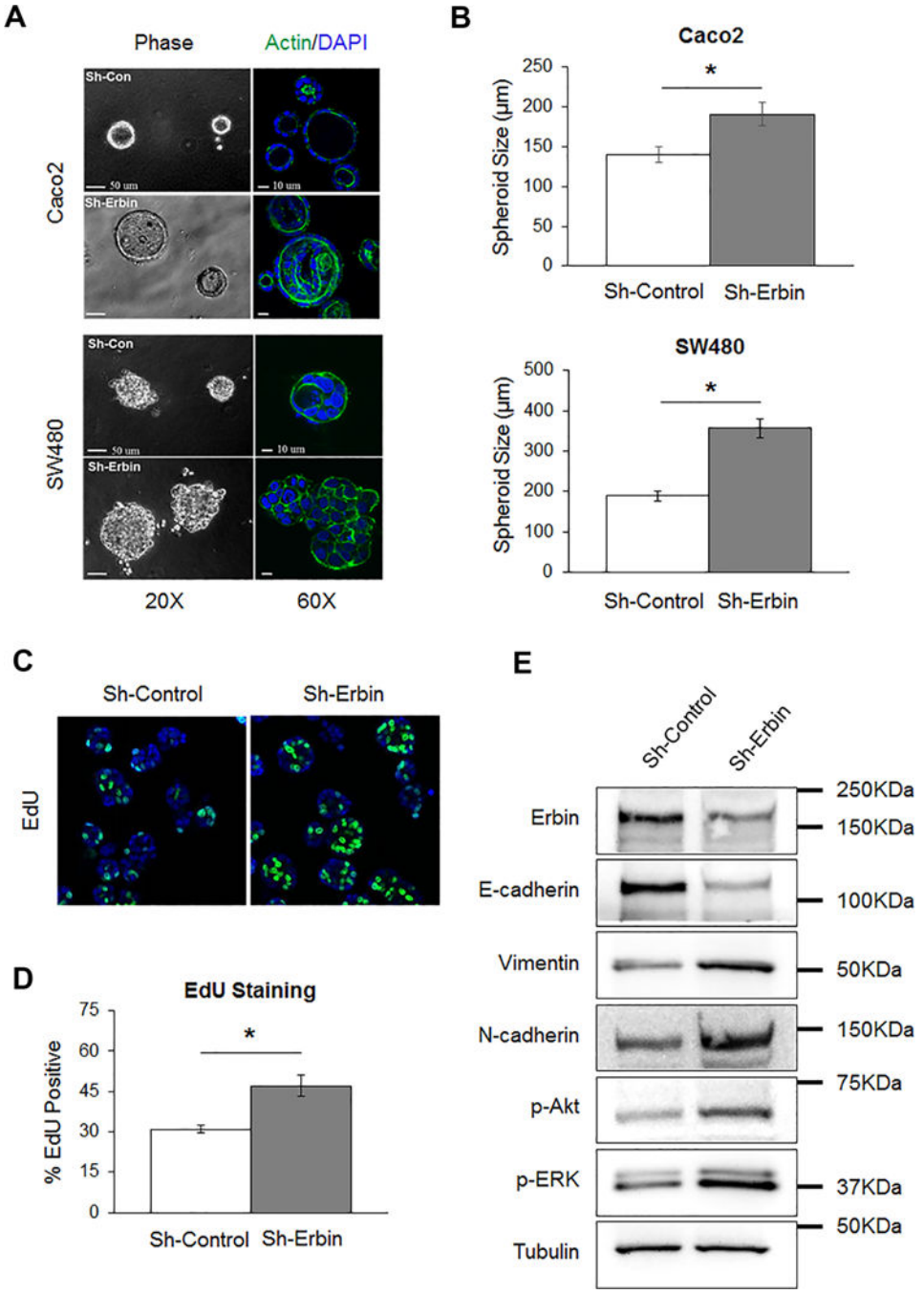

Figure 3. Knockdown of Erbin disrupts epithelial cell polarity.

(A) Stable sh-Control and sh-Erbin Caco2 and SW480 cells were cultured for 10 days in 3D Matrigel. IF images were taken from cells stained with Alexa488-phalloidin (green) and DAPI (blue). Phase-contrast images were obtained using a Nikon TE2000 inverted microscope with 10X objective, scale bar, 50µm; and confocal images of stained cells were obtained using an Olympus FlowView FV1000 confocal laser-scanning microscope, scale bar, 10µm. (B) The diameter of 15–35 randomly chosen spheroids of sh-Control and sh-Erbin Caco2 and SW480 cells were measured. Data represents the mean ± SEM (* $p<0.05$).

(C) Stable sh-Control and sh-Erbin SW480 cells were labeled with EdU to mark proliferating cells. (D) The percentage of EdU-positive cells were quantified and expressed graphically. Data represents mean ± SEM (* $p<0.05$). (D) Stable sh-Control and sh-Erbin SW480 cells were cultured for 10 days in 3D Matrigel and spheroids were collected and analyzed by western blot for the expression of EMT markers.

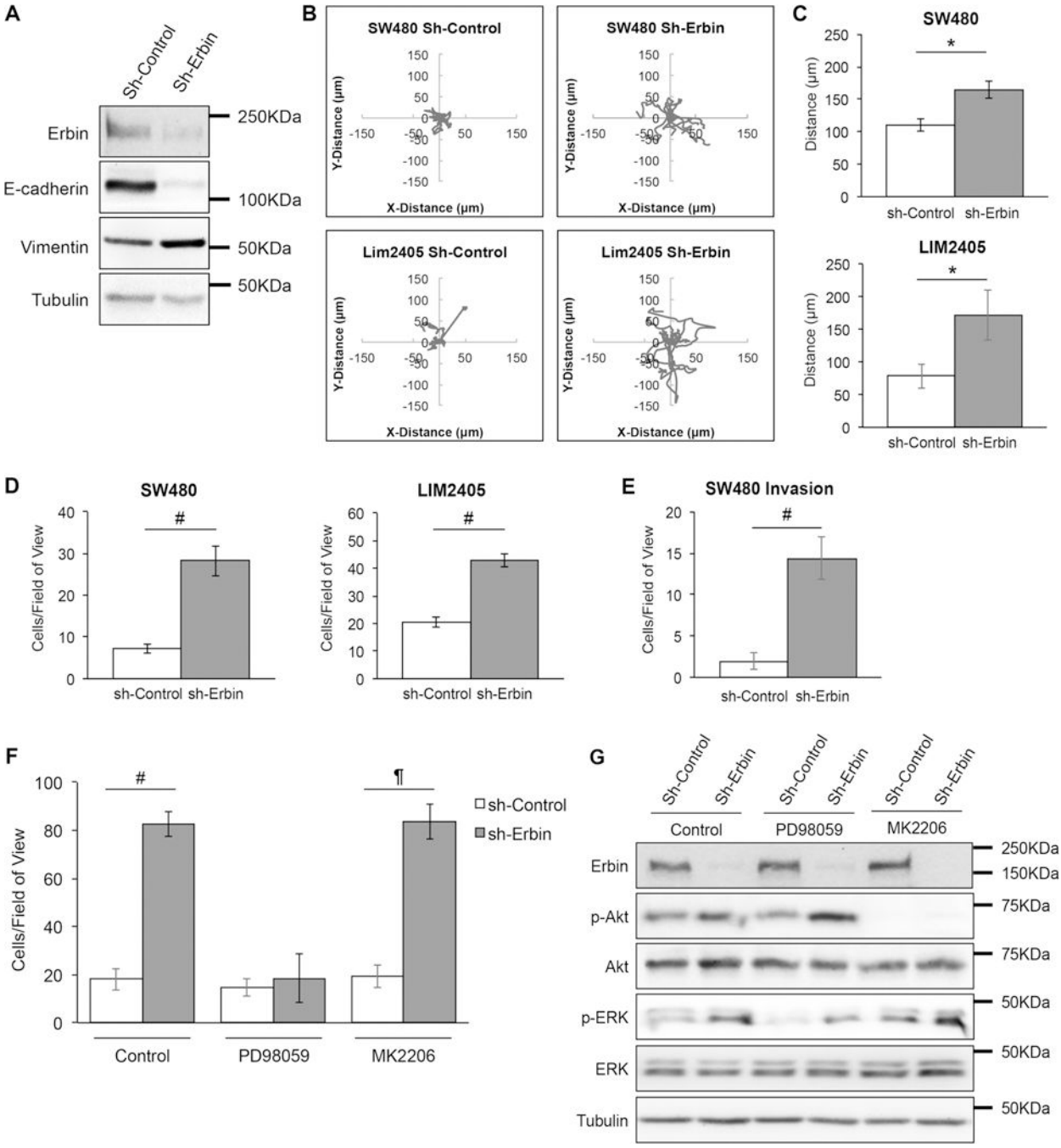

Figure 4. Knockdown of Erbin increases cell motility in CRC cells.

(A) Stable sh-Control and sh-Erbin SW480 cells grown in 2D culture were analyzed for the expression of Erbin, E-cadherin and Vimentin. (B) Migration paths of stable sh-Control and sh-Erbin SW480 and LIM2405 cells were monitored using the Nikon Biostation for 6 hours. The trajectories of 12 randomly chosen cells for each cell line were shown in the graphs. (C) The averaged path lengths were quantified for sh-Control and sh-Erbin LIM2405 and SW480 cells. Data represents mean ± SEM (* $p<0.05$). (D) Stable sh-Control and sh-Erbin SW480 and LIM2405 cells were subjected to Transwell migration assays using collagen and

EGF (10 ng/mL) as chemoattractants. The number of migrated cells per field of view were counted. Data represents mean ± SEM (n=12, # $p<0.0001$). (E) Stable sh-Control and sh-Erbin SW480 cells were subjected to Transwell invasion assays using 5% FBS as the chemoattractant. The number of invaded cells per field of view were counted. Data represents mean ± SEM (# $p<0.0001$). (F) Stable sh-Control and sh-Erbin SW480 cells were treated overnight with MEK inhibitor PD98059 (10 μM) or Akt inhibitor MK2206 (1 μM), and subsequently subjected to Transwell migration assays using collagen and EGF (10 ng/mL) as chemoattractants. The number of migrated cells per field of view were counted. Data represents mean ± SD (# $p<0.001$ and ¶ $p<0.01$). (G) Cell lysates were prepared from sh-Control and sh-Erbin SW480 cells as treated in (F) and analyzed for the phosphorylation of Akt and ERK using western blot.

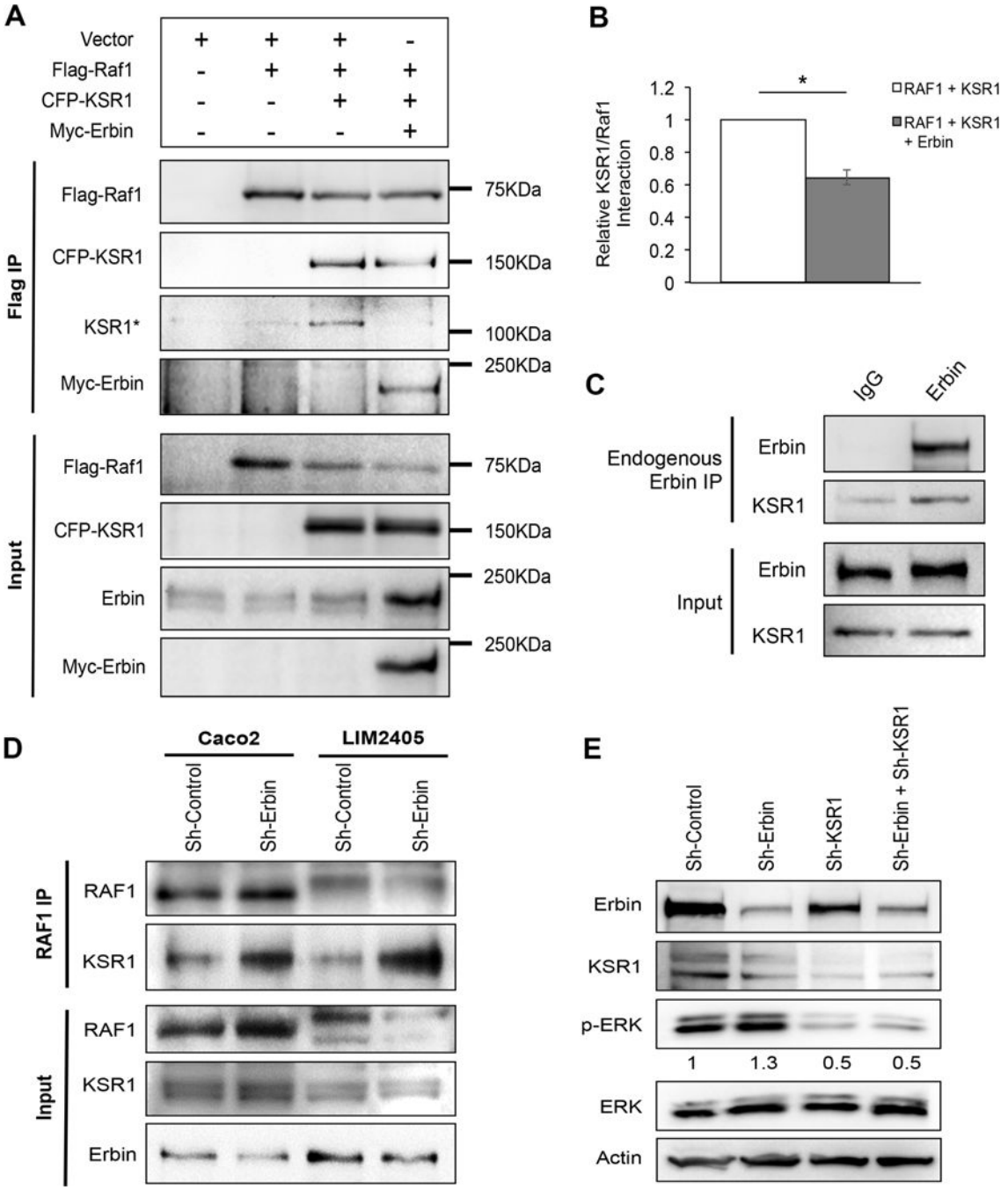

Figure 5. Erbin disrupts the interaction between KSR1 and RAF1.

(A) 293T cells transfected with Flag-RAF1 and CFP-KSR1 in the presence or absence of Myc-Erbin co-expression were lysed and immunoprecipitated with Flag-affinity beads. The presence of KSR1 and Erbin in the immunoprecipitates were detected by Western blot. The arrow indicates the endogenous KSR1 co-immunoprecipitated by Flag-RAF1. (B) The relative amount of KSR1 co-immunoprecipitated with RAF1 in the presence or absence of Myc-Erbin co-expression was quantified and expressed graphically (n=3, * $p<0.05$). (C) Erbin interacts with endogenous KSR1. Endogenous Erbin was immunoprecipitated from

LIM2405 cell lysates and the presence of KSR1 in the immunoprecipitates was detected by Western blot. (D) Endogenous RAF1 was immunoprecipitated from sh-Control and sh-Erbin Caco2 and LIM2405 cells. The levels of KSR1 co-immunoprecipitated with RAF1 were detected by Western blot. (E) The expression of KSR1 and Erbin were silenced individually or in combination in SW480 cells using corresponding shRNA lentivirus. Cell lysates were analyzed for the phosphorylation status of ERK. The relative levels of ERK phosphorylation in different cells were quantified by normalizing ECL signals generated by p-ERK to that of total ERK.

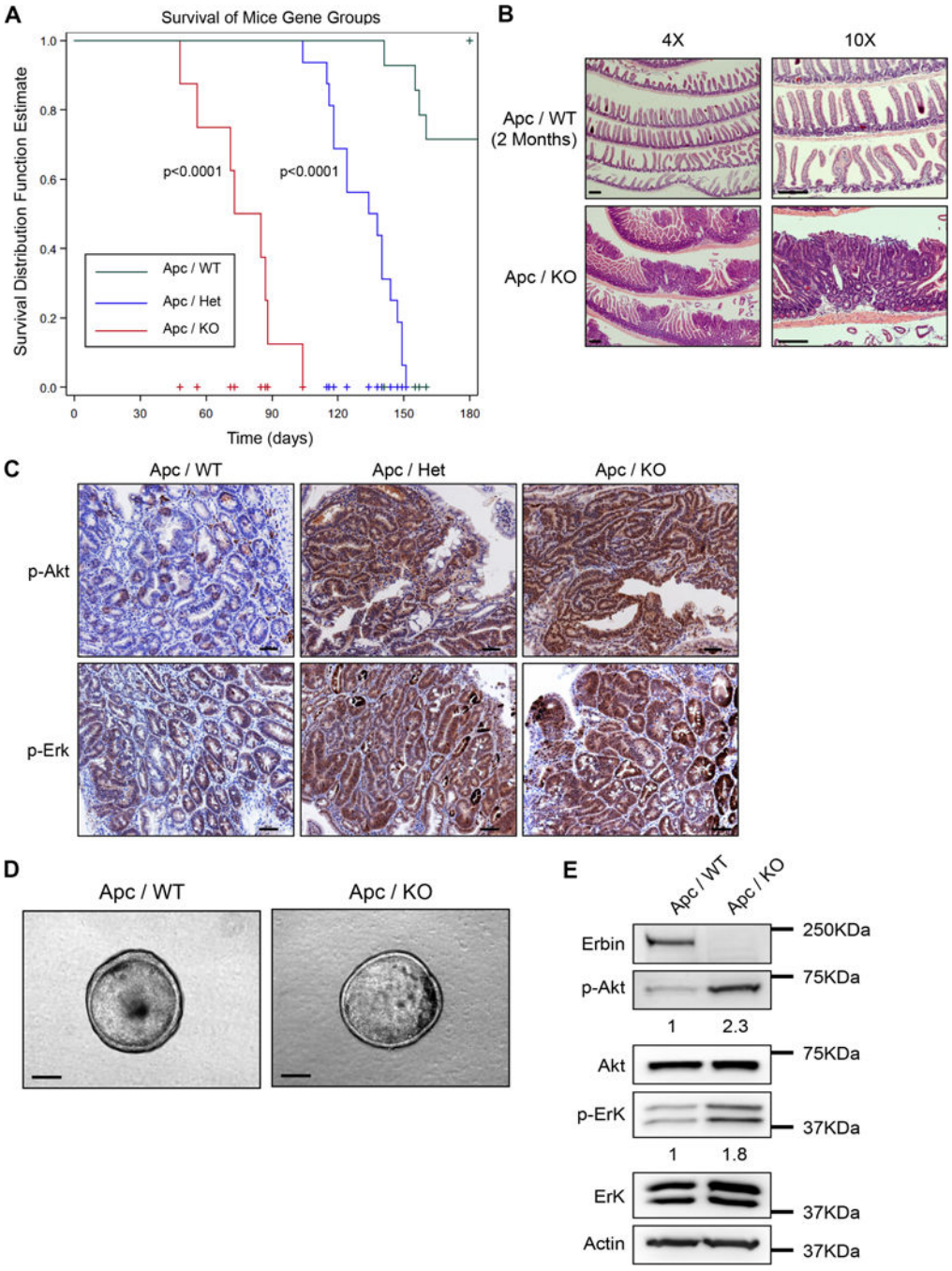

Figure 6. Erbin deletion decreases survival and promotes the activation of Akt and Ras/Raf signaling in Apc mutant mice.

(A) Erbin-loss significantly reduces the lifespan of Apc mutant mice. Kaplan-Meier curve shows the survival distribution of three cohorts of mice: $Apc^{f/+}$/Vil-Cre/$Erbin^{+/+}$, $Apc^{f/+}$/Vil-Cre/$Erbin^{+/-}$ and $Apc^{f/+}$/Vil-Cre/$Erbin^{-/-}$ (Apc/WT, Apc/Het, and Apc/KO, respectively). Numbers of mice in the three cohorts are: Apc/WT (n=14), Apc/Het (n=16) and Apc/KO (n=8). Statistical significance (determined by Log Rank test) is given for comparison between Apc/WT and Apc/Het ($p<0.0001$) and Apc/WT and Apc/KO ($p<0.0001$). (B) Histology analysis of intestine adenomas in age-matched Apc/WT and Apc/KO mice (at 2

months). Scale bar, 200μm. (C) The phosphorylation of Akt and Erk was analyzed in the intestinal tumors from Apc/WT, Apc/Het, and Apc/KO mice using IHC staining. The tissues were collected when the mice were at the terminal stage of tumor development. The age of the mice was 4.5 months for Apc/WT and Apc/Het and 2 months for Apc/KO mice, respectively. Scale bars, 50 μm. (D) Tumor organoids were prepared from tumor tissues of Apc/WT and Apc/KO mice and grown in 3D Matrigel. Scale bar, 200μm. (E) Cell lysates were prepared from tumor organoids as shown in (D) and analyzed for the phosphorylation status of Akt and ERK by western blot. The relative levels of Akt and ErK phosphorylation were quantified by normalizing ECL signals generated by p-Akt and p-ErK to that of total Akt and ERK, respectively.

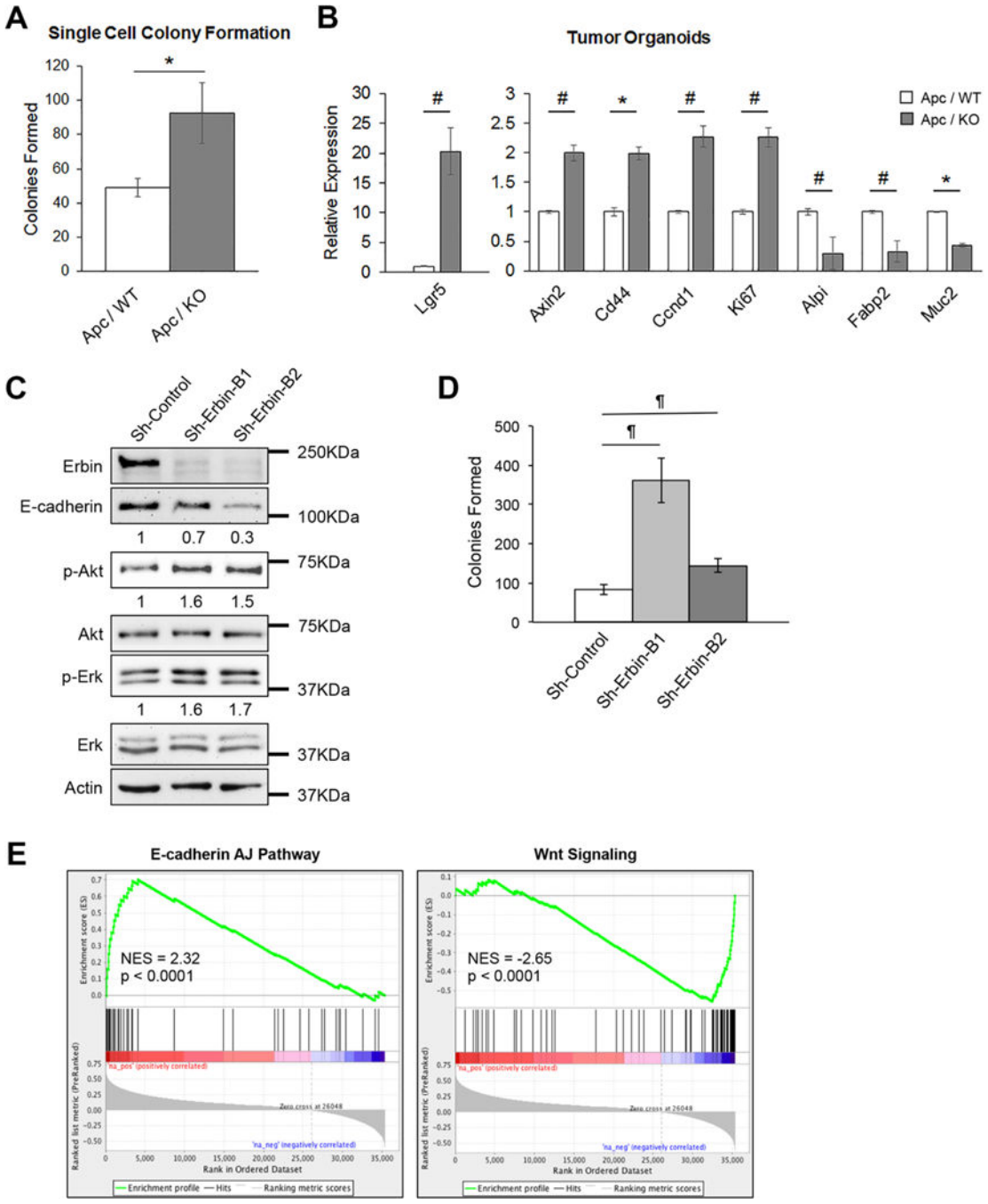

Figure 7. Loss of Erbin enhances tumor initiation properties in tumor organoids.

(A) Tumor organoids derived from Apc/WT and Apc/KO mice were dissociated into single cells and 1,000 cells were reseeded in 3D Matrigel. The number of cells that were able to successfully form colonies were quantified. Data represents mean ± SEM (* $p<0.05$). (B) Tumor organoids derived from Apc/WT and Apc/KO mice grown in 3D Matrigel for 72 hours were collected and analyzed for the expression of Wnt target genes (Lgr5, Axin2 and Cd44), cell proliferation (Ccnd1 and Ki67) and intestinal differentiation (Alpi, Fabp2 and Muc2) using quantitative RT-PCR. Two different mice of each genotype were used to

prepare tumor organoids. RT-PCR analyses were performed separately with tumor organoids from individual animal and results are combined and summarized in the bar graphs. Data represent mean ± SEM (# $p< 0.0001$ and * $p<0.05$). (C) Tumor organoids derived from Apc/$Kras^{G12D}$ double mutant mice were infected with control and sh-Erbin lentivirus (B1 and B2) and selected to obtain stable Erbin knockdown tumor cells. Protein lysates prepared from control and Erbin knockdown tumor organoids grown in 3D and analyzed for the expression of Erbin and E-cadherin and the phosphorylation of Akt and Erk. The relative levels of Akt and Erk phosphorylation were quantified by normalizing ECL signals generated by p-Akt and p-Erk to that of total Akt and Erk, respectively. (D) Control and Erbin knockdown Apc/$Kras^{G12D}$ tumor organoids were dissociated into single cells and 1,000 cells were reseeded in 3D Matrigel. The number of cells that were able to successfully form colonies were quantified. Data represents mean ± SEM (¶ $p<0.01$). (E) The Gene Set Enrichment Analysis (GSEA) was performed using the TCGA CRC RNA-seq dataset to identify genes that have positive or negative correlations with Erbin expression. Enrichment plots showed significant correlation of the E-cadherin pathway (NES = 2.32, FDR <0.0001) and Wnt signaling (NES = –2.65, FDR <0.0001) with Erbin expression in CRC patients.